Nanoscale Advances

ROYAL SOCIETY OF CHEMISTRY

PAPER

View Article Online
View Journal | View Issue

Cite this: *Nanoscale Adv.*, 2025, **7**, 4721

Study of the impact of photonic crystal additives on the piezoresponse of PVDF nanofibers

Qianqian Zhang,† Neha Yadav,† Yongling Wu, * Ashish Yadav * and Zheng Hongyu *

Piezoelectric nanocomposites have been a rapidly growing field in energy harvesting, with applications in wearable electronics, strain sensors, mechanical actuators, and electromechanical membranes. This research initially reported the use of three-dimensional polymer photonic crystals with varying ratios. PVDF is responsible for piezoelectric performance and is a promising polymeric organic material for converting applied mechanical stress into electric voltage. In addition, TPU is widely used in the plastic industry due to its superior elasticity. Our work investigates the piezoelectric response of different blending ratios of PC + PVDF/TPU. it has been found that higher ratio of PC give higher output voltage under different stress conditions and higher photosensitivity. Then, addition of TPU, owing to its superior mechanical elasticity, can partially compensate for PVDF to enhance the piezoelectric response of the PVDF/TPU nanocomposite mats. This work can help increase strain sensitivity and mechanical elasticity with PCs, making it a unique contribution in this research direction and valuable for future devices.

Received 13th May 2025
Accepted 10th June 2025

DOI: 10.1039/d5na00474h

rsc.li/nanoscale-advances

Introduction

Flexible piezoelectric films have enormous potential in applications ranging from biomimetics, sensors, memory, and energy harvesting.[1–3] Poly(vinylidene fluoride) (PVDF) is an organic polymer that can be solution-processed to form flexible films that exhibit ferroelectric, piezoelectric, and pyroelectric properties. PVDF offers many advantages in emerging applications as it does not contain metals or toxic elements and is mechanically robust, flexible, lightweight, and even biocompatible.[4,5] It has five crystalline polymorphs (α–ε), resulting in a high degree of diversity and customizability in material properties and response *via* dedicated fabrication protocols.[6–8] The antiparallel packing of dipoles in the α and ε PVDF phases leads to non-polar, insulating films, while the β, γ, and δ phases are polar and exhibit piezo, pyro, and ferroelectricity.[6,7] The β-phase is less thermodynamically favorable than the α-phase but demonstrates the most robust piezoelectric response of all five phases. Therefore, much effort has been dedicated to increasing the β-phase yield in PVDF films and to potential applications of piezoelectric β-phase PVDF.[9,10] A challenge for PVDF piezoelectric applications is the lack of relevant fabrication protocols for industrial-scale production. In research laboratories, PVDF is commonly fabricated using drop-casting, spin-casting, electrospinning, or Langmuir–Blodgett, combined with mechanical or electrical stress in post-processing steps to improve the β-phase yield.[11–13] Further, chemical derivatives of PVDF, such as PVDF-TrFE, suppress the formation of the α-phase through the steric hindrance of neighboring chains while supporting the formation of the β-phase, thereby reducing the need for post-processing. Additive manufacturing (AM) has recently emerged as an alternative fabrication route for low-cost prototyping and production of sophisticated structures beyond planar thin films. AM processes use heat, light, and/or chemical reactions to convert adhesives into tailored geometries. Photonic crystals (PCs) have unique properties.[14–16]

Here, we demonstrate a proof-of-concept for the 3D printing of piezoelectric PVDF-TPU + PC films. The photochemical PVDF-TPU-PC-based liquid resin is converted into a piezoelectric[17,18] 3D structured film within a single printing step. Electrospinning also provides the ability to further enhance the piezoelectric properties of the fabricated PVDF nanofibers, as it enables the production of aligned fibers with hollow structures or various additives for improved performance.[19] Such additives include carbon nanotubes (CNTs), graphene, and ZnO.[20,21] Furthermore, PVDF and its copolymers have been utilized for pressure sensing applications, serving as healthcare monitoring devices for respiration signals. Composites of PVDF and graphene oxides have also been developed for multiple sensory applications, exhibiting high sensitivity for monitoring simultaneous artery pulse pressures and temperatures.[22] Due to their excellent flexibility, PVDF nanofibers have also been explored for blood pressure sensors.[23–25]

Our work analyzes the detailed mechanical and piezoelectric characteristics of different blending ratios of PVDF and TPU

Center for advanced laser manufacturing (CALM), Shandong university of technology, Zibo, 255000, P.R. China. E-mail: zhenghongyu@sdut.edu.cn; ashish@sdut.edu.cn; wuyl2019@sina.com

† These authors contributed equally.

nanofiber combinations of PC mats synthesized by the electrospinning process. Specifically, we investigate the optimum blending ratios to generate the maximum voltage at varying applied forces. In addition, we show the impact of the frequency of the applied force on the piezo-response behavior of different blended nanofiber mats. This work is helpful for wearable electronics and energy harvesting units.

Experimental work

Materials

ARKEMA Shanghai supplies polyvinylidene fluoride (PVDF) (Kynar 716 A) and has an average M_w equal to 3×10^5, which was purchased from Arkema Shanghai Distribution Co., Ltd. Thermoplastic polyurethane (TPU) with a polydispersity index (PDI) of 1.83 and a molecular weight of 107 020 g mol^{-1} is provided by BASF Co., Ltd, Berlin, Germany. Polymer concentrations have been dispersed in dimethylformamide (DMF 98%, Sigma-Aldrich, Taufkirchen, Germany). Two solvents were prepared with ace : DMF (volume ratio 3 : 2). One bottle was heated to 80 °C, and TPU (15% wt) was added and stirred at 600 rpm until completely dissolved. The other bottle was heated to 50 °C, and PMMA photonic crystals with different proportions were added, dispersed evenly, and then PVDF (15% wt) was added at 60 °C and 600 rpm until entirely soluble. The two solutions were mixed 1 : 1.

Membrane fabrication

Different blending ratios of PVDF/TPU and PC solution with a constant polymer concentration were prepared and processed through the electrospinning setup. A comparative study of the effect of PC addition on the piezoelectric and mechanical properties of the PVDF mat was conducted. The electrospinning process was performed by adding 10 mL of polymer solution into a plastic syringe tipped with a stainless-steel needle. The positive voltages were provided from a high voltage power supply CZE1000R to the metallic needle with gauge 18, for application of voltages around 25 kV with a constant feed rate of 1 mL h^{-1} using a NE1000 syringe pump (New Era Pump Systems, Suffolk County, NY, USA). The needle-to-collector distance was adjusted to 10 cm. A random PVDF/TPU/PC nanofiber composite was collected on a drum collector covered with aluminum foil and connected to the ground.

Piezoelectric characterization

The synthesized PVDF/TPU nanofiber membranes underwent evaluation under cyclic loading using a custom-designed excitation device (refer to Fig. 1). This apparatus incorporates a lightweight spring plunger mechanism that oscillates vertically. The excitation frequency is modified by changing the speed of the brushless DC motor that drives the plunger, with the assistance of an electronic speed controller. The sample is positioned between two foil sheets, which are connected through shielded wires to a high-impedance oscilloscope (Tektronix MDO3014), and is situated beneath the plunger. The maximum load applied is controlled by adjusting the plunger's height, which alters the spring's compression distance when it interacts with the sample during the process.

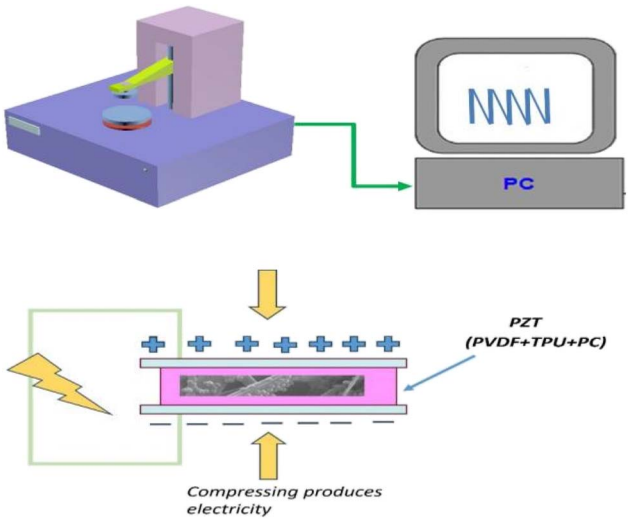

Fig. 1 Schematic representation of the piezoelectric characterization set-up and a picture of the accurate set-up.

Results and discussion

Morphological characterization

Fig. 1 shows the measurement of the strain sensing instrument used to test the samples and the basic experimental setup. The morphology of the nanofibers was observed using a scanning electron microscope at an accelerated voltage of 20 kV. The film is placed on a short aluminum column, fixed with conductive carbon tape, and sprayed with gold to make it fully conductive. SEM analysis was used to examine the morphology and size of the nanofibers, and the images are shown in Fig. 2. With photonic crystal particles attached to the surface, the adequate particle size of the photonic crystals was approximately 240 nm. Based on the SEM image analyses, the adhesion of photonic crystals to the surface of PVDF/TPU nanofibers is confirmed. N. Shehata *et al.* reported that mechanical elasticity supports the piezoelectric response.[26,27] In our case, we enhanced the performance with the help of a 3D photonic crystal.

Fig. 2 shows the SEM image distribution of the composite nanofibers. ImageJ was used to calculate the average fiber diameter of the nanofibers in all samples. The image indicates that the photonic crystals are uniformly distributed in the fibers. The histogram of the diameter distribution of the photonic crystal composite fibers is shown in Fig. 2. The results show that the average fiber diameter of the TPU/PVDF composite fibers ranges from 500 to 1200 nm; it is observed that the addition of photonic crystals has no significant effect on the fiber diameter, ensuring the high compatibility and uniformity of the mixed polymer solution. The photonic crystals are well-arranged along the fiber.

Fig. 3 shows the SEM images of PVDF/TPU composite nanofibers and PVDF/TPU/PC composite nanofibers. The photos display homogeneous fiber distribution with minimal

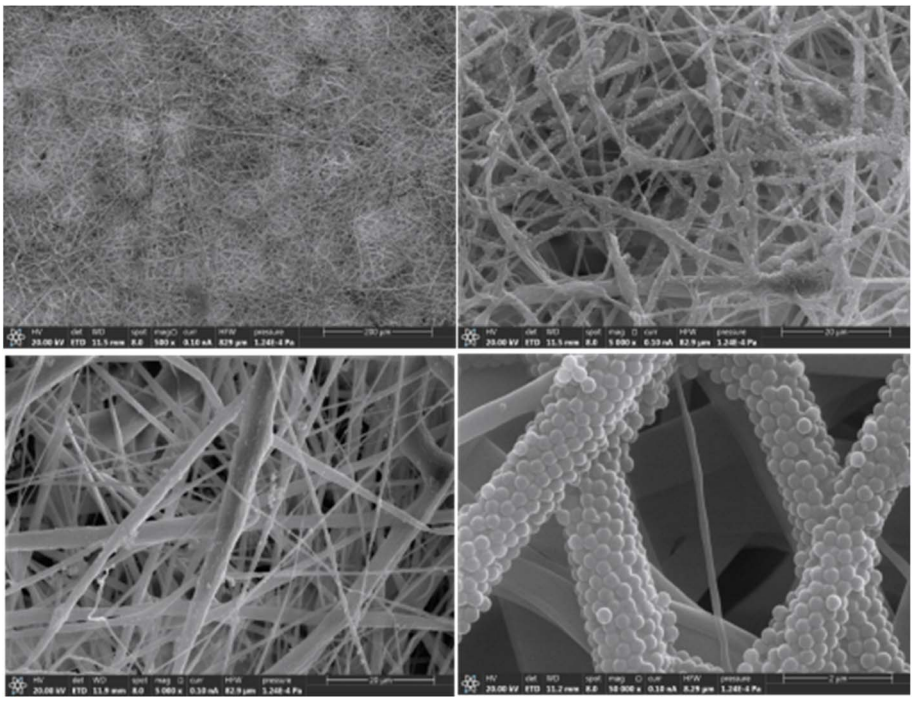

Fig. 2 The SEM image distribution of PVDF/TPU composite nanofibers and the attachment of a photonic crystal to the fiber.

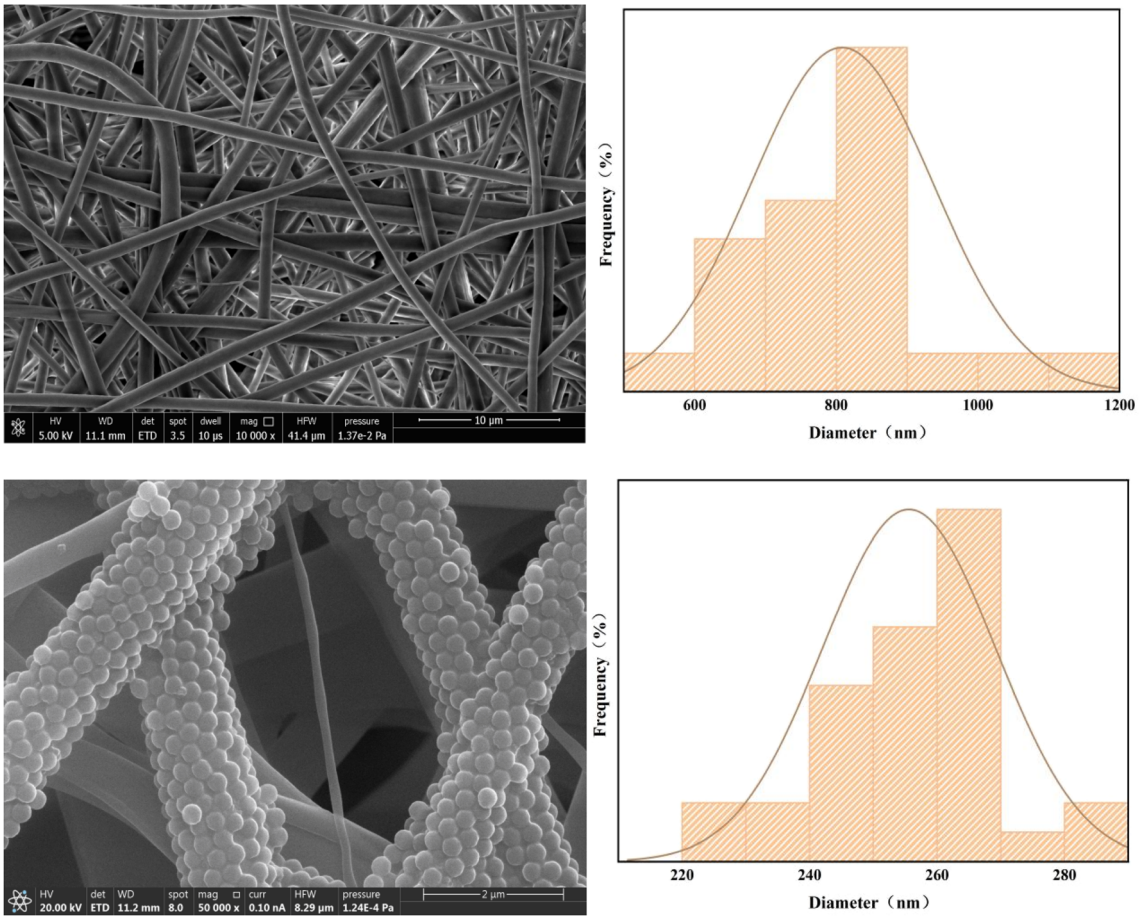

Fig. 3 Homogeneous fiber distribution of PVDF/TPU & attachment with photonic crystals.

bead formation. The average fiber diameter was calculated, and a histogram of the fiber distribution is presented in Fig. 3. The results indicate an average fiber diameter of 254 nm to 267 nm for pure PVDF and blended composite mats. It was observed that the addition of TPU didn't significantly affect the fiber diameter, ensuring the high compatibility and homogeneity of the mixed polymer solution.

Physical characterization

The FT-IR spectra of nanofibrous composite membranes are shown in the Figure. The FT-IR data are introduced to identify the crystalline phases of PVDF. PVDF can be formed in five crystalline polymorph phases (α, β, γ, δ, and ε). The α-phase is considered the most common and stable non-polar phase of PVDF, while the β-phase content is an essential prerequisite for enhancing the piezoelectric properties. Through the electrospinning process, the high electric field induces the dipoles to be aligned in the same direction normal to the chain axis. This crystal form can, therefore, generate the most considerable spontaneous polarization and exhibit a strong piezoelectric effect. Thus, the β-phase is the most critical phase for piezoelectric and pyroelectric applications.[28–30]

As shown in Fig. 4, the graph shows the leading characteristic bands for PVDF at 840 cm^{-1} for CH_2 rocking, C–C and CF_2 stretching, and 1175 and 1400 cm^{-1} for C and C vibrations, respectively. The characteristic bands of TPU appeared at 1533, 1735, 2971, and 3365 cm^{-1}, corresponding to the –CONH— asymmetrical bond, C═O, C–H, and N–H stretching, respectively.[31,32]

Moreover, with the addition of photonic crystals, the position of each absorption peak remains unchanged, but the intensity and shape of the peak change. The β-phase absorption pattern of PVDF/TPU nanofibers at 840 cm^{-1} is substantial and increases with the increase in photonic crystal concentration,[33,34] which is consistent with the decrease in piezoelectric response due to the addition of photonic crystals. The relative amount of β phase has been quantified by considering the

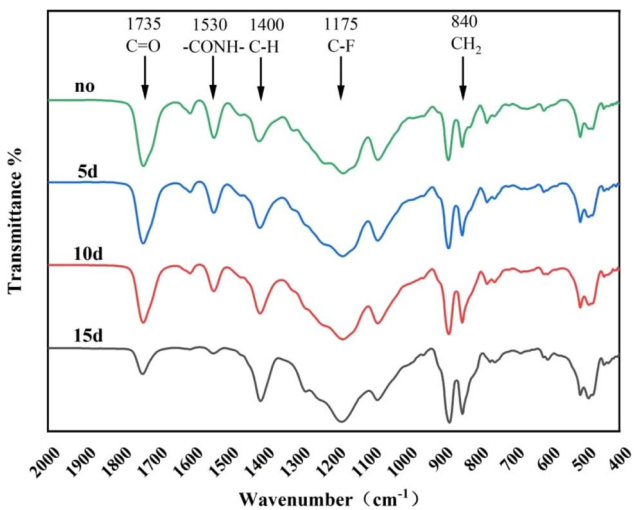

Fig. 4 FT-IR curves for PVDF/TPU/PC composite nanofibers.

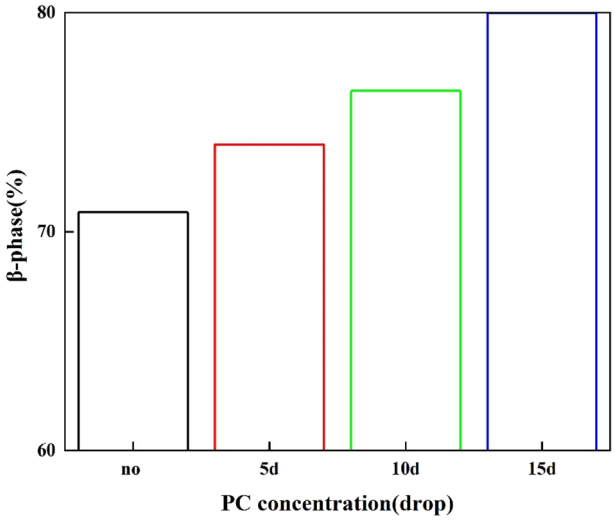

Fig. 5 The β-phase of nanofibers with different PC concentrations.

relative absorption intensity of the β phase at 840 cm^{-1} and the α phase at 760 cm^{-1} according to the proposed equation by Gregorio and Cestari:

$$F(\beta) = \frac{A_\beta}{(K_\beta/K_\alpha)A_\alpha + A_\beta} \times 100\%$$

where $F(\beta)$ is the relative fraction of the β-phase, A_β is the absorbance at 840 cm^{-1}, and A_α is the absorbance at 760 cm^{-1}. The K_α and K_β represent the absorption coefficients at the corresponding wavenumbers, which are 6.1 × 104 cm^2 mol^{-1} and 7.1 × 104 cm^2 mol^{-1}, respectively.

The β-phase content $F(\beta)$ of the nanofiber membranes can be calculated.[35,36] Fig. 5 quantitatively shows the β-phase content of the four PVDF-based fiber membranes. The $F(\beta)$ of the untreated pure PVDF/TPU is 70.89%, and it keeps increasing with the increase of the photonic crystal content. The $F(\beta)$ of the PVDF/TPU/5d PC membrane reaches 73.98%, that of the PVDF/TPU/10d PC membrane reaches 76.44, and that of the PVDF/TPU/15d PC membrane reaches 79.99%. The addition of 15d PCs is 88.62% of the pure PVDF/TPU. This further proves that a small amount of nano-fillers are widely used to stimulate nucleation to promote the process of β-phase formation in PVDF-based polymers. This is due to the fact that the positive charge on the $–CF_2$ group of the PVDF molecular chain attracts the negative charge carried by the particles and the fillers form a local electric field that is conducive to the transformation into the β-phase.

Mechanical properties

To further investigate the impact of incorporating nanoparticles on the tensile properties of membrane, the tensile properties. Fig. 6 presents the mechanical properties of the four membranes (stress–strain curve graph), among which the elongation at break of the composite film containing photonic crystals is higher than that of the PVDF/TPU film. During the stretching stage, the elastic deformation curves of all samples

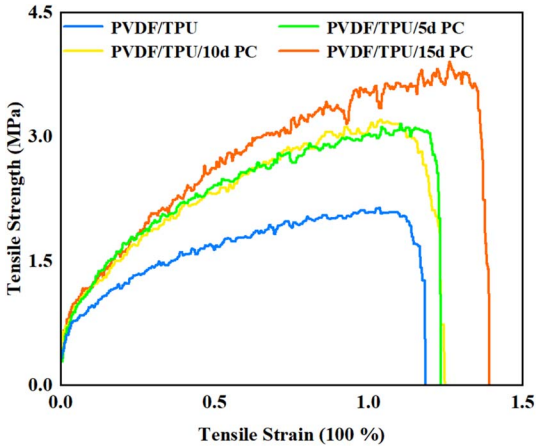

Fig. 6 Tensile strength–strain curves of four types of nanofibers with different PC concentrations.

showed good linearity, indicating that the films have a stable elastic deformation capacity. All curves exhibit the following trend: ascending section (elastic/plastic deformation) → peak (maximum tensile strength) → descending section (material fracture).

In the ascending section, as the strain increases, the stress gradually rises, which reflects the material's ability to resist deformation. At the peak point, the highest point of the curve corresponds to the material's maximum tensile strength (*i.e.*, the maximum stress the material can withstand before fracture), which is a key indicator of the material's mechanical properties. In the descending section, the stress drops sharply, indicating the material's failure due to fracture.

The strain at this point corresponds to the fracture strain (*i.e.*, the maximum deformation capacity of the material before fracture). For the PVDF/TPU samples, their maximum tensile strength is the lowest (approximately 2 MPa), and the fracture strain is the smallest (approximately 1.1), indicating that the mechanical properties of this base system are relatively weak. The strength and strain of the PVDF/TPU/5d PC and PVDF/TPU/10d PC systems are both higher than those of the base system, and the performance of the PVDF/TPU/10d PC system is slightly better than that of the PVDF/TPU/5d PC system. This indicates that the addition of photonic crystals can enhance the mechanical properties of the material, and there is a certain optimization range. The PVDF/TPU/15d PC system has the highest tensile strength (approximately 4 MPa) and the largest elongation at break (approximately 1.4), demonstrating the best mechanical properties among the four systems. This indicates that a higher PC addition amount (15d) has a significant effect on enhancing the strength and toughness of the material.

Piezoelectric characterization

An electrospinning device was used to prepare the composite nanofiber film, which was then cut into a 3 cm × 3 cm square. Copper and silver electrodes were wrapped around the sample to create a device with sensing performance, and the entire assembly was completely encapsulated in a PI film. As schematically shown in Fig. 7a, a series of output signals was collected from the PENG using an independently built sensing test platform, including mechanical supports, voice coil motors, conversion circuits, and digital acquisition equipment. Fig. 7b shows the composite fiber fabrication.[28,29]

It can be concluded that without the addition of photonic crystals, the voltage fluctuates around 0, with a relatively small amplitude, with peaks approximately at 4 V and troughs approximately at −4 V, showing a relatively regular periodic fluctuation. When five drops of photonic crystals are added, the amplitude of voltage fluctuation significantly increases, with peaks approximately at 7 V and troughs approximately at −7 V, still showing periodic volatility but with a higher overall voltage value. When 10 drops of photonic crystals are added, the amplitude of voltage fluctuation further increases, with peaks approximately at 17 V and troughs approximately at −17 V. The periodic fluctuation still exists, with the voltage value higher than that at five drops. When 15 drops of photonic crystals are added, the amplitude of voltage fluctuation is the largest, with peaks approximately at 27 V and troughs approximately at −27 V. The periodic fluctuation pattern is similar, but the voltage value reaches its highest. In summary, as the amount of photonic crystals increases, the amplitude of voltage fluctuation gradually increases, and both the peaks and troughs keep rising, indicating that the piezoelectric performance of the system changes significantly under different photonic crystal content conditions.

Fig. 8 shows that the piezoelectric nanogenerator (PENG) exhibits repeatable and stable voltage output performance. Compared to the PVDF/TPU composite system, the PVDF/TPU/PC PENG demonstrates significantly enhanced voltage output capability. Notably, the output voltage of the PVDF/TPU/15d PC-PENG reaches approximately 25 V, representing an increase of ∼21 V (∼525% or ∼6.25 times) over the PVDF/TPU reference sample (4 V). This confirms that the incorporation of photonic

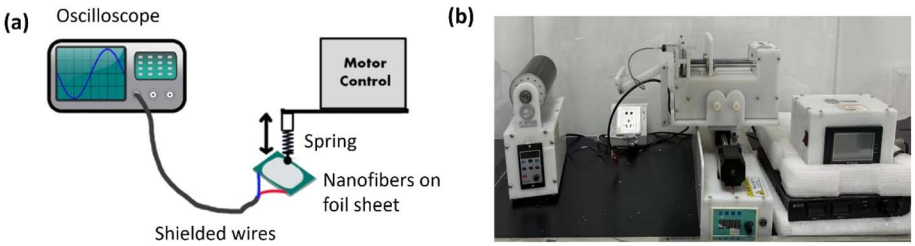

Fig. 7 Schematic representation of the piezoelectric characterization set-up (a), and a picture of the accurate set-up (b).

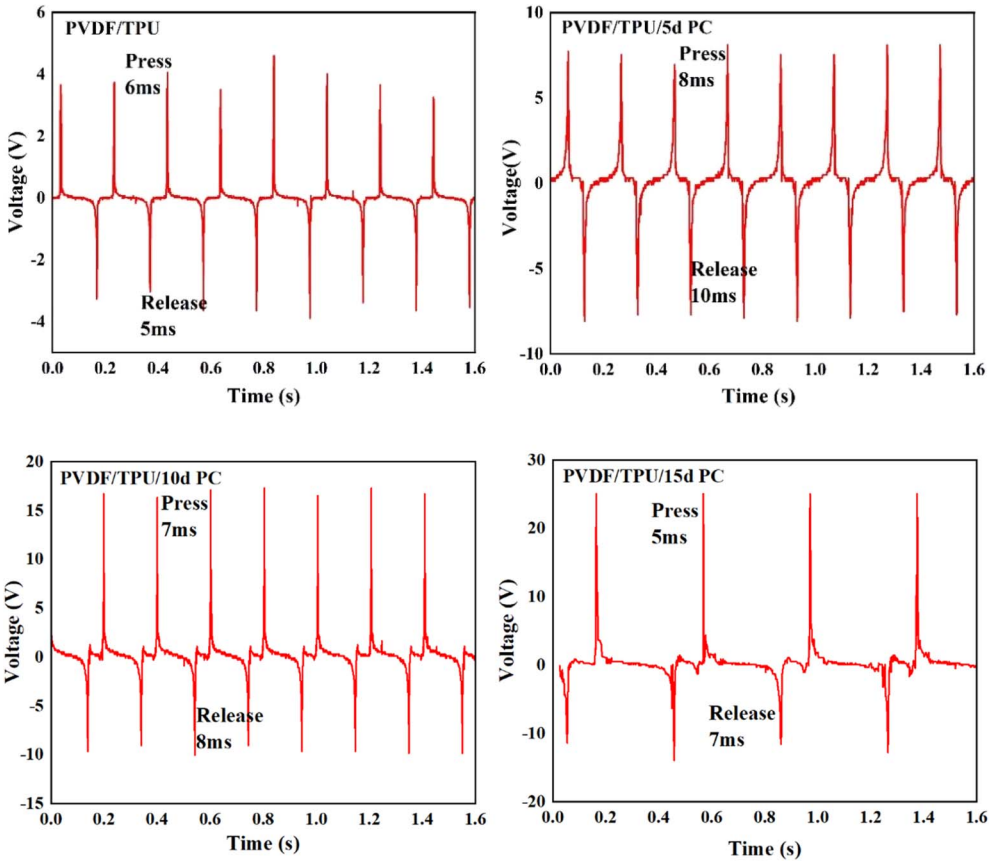

Fig. 8 Strain sensing measurements with different concentrations of photonic crystals, *i.e.*, 0%, 5d, 10d, and 15d.

crystals (PCs) effectively enhances the piezoelectric performance of the PENG.

Regarding dynamic response characteristics, the PVDF/TPU exhibits response/recovery times of 6/5 ms. As the PC microsphere content increases, the response/recovery times of the PENG initially increase and then decrease, though the overall variation range is limited. At lower PC content (*e.g.*, PVDF/TPU/5d PC-PENG), the response/recovery times extend to 8/10 ms. This variation is attributed to the enhanced piezoelectric synergistic effect between the PC microspheres and the β-phase PVDF matrix, leading to an increased total accumulated charge and prolonged charge accumulation process. However, with further increase in PC microsphere content (*e.g.*, PVDF/TPU/15d PC), the synergistic enhancement effect weakens, and the response/recovery times shorten to 5/6 ms. It should be noted that the recovery time of PENGs is typically longer than the response time, while the introduction of PC microspheres improves the surface elasticity, facilitating rapid recovery and elimination of deformation.

Mechanistic studies reveal that the micro-nano structure of the photonic crystal induces localized high strain in critical regions of the piezoelectric material through stress/strain concentration effects, thereby directly amplifying the piezoelectric output signal. This mechanism, combined with the aforementioned piezoelectric synergistic effect, collectively contributes to the performance enhancement of the PENG.

As shown in Fig. 9, the relationship between frequency and output voltage is demonstrated, as well as the influence of different frequencies on the output voltage under the same force. As shown in Fig. 9a, all the curves present the rule that the voltage increases with the increase of frequency, indicating that under the test conditions, the higher the frequency, the stronger the voltage signal generated by the material, reflecting the positive correlation between frequency and voltage. When only PVDF/TPU is used, its output voltage is the lowest. When the frequency reaches the maximum, the output voltage reaches 5 V. With the increase of the addition amount of PCs, the output voltages of different samples at the same frequency increase, which indicates that the increase of PCs has a positive response to the output voltage. When the addition amount is 15 drops of PCs, its output voltage reaches a maximum of about 16 V, which indicates that the increase of PCs enhances the piezoelectric performance. As shown in Fig. 9b, it can be found that under the action of a force of 10 N, the output voltage of the sample varies between 3 and 20 v within the range of 1–11 Hz, and the PENG has stable performance output at different frequencies. As shown in Fig. 9c, under the frequency of 5 Hz, within the force range of 3–32 N, the output voltage of the sample is in the range of 3–25 V. As the force increases, the output voltage shows a slow and stable growth trend, with the voltage amplitude stably output. This indicates that the PENG has a stable performance output under different force applications.

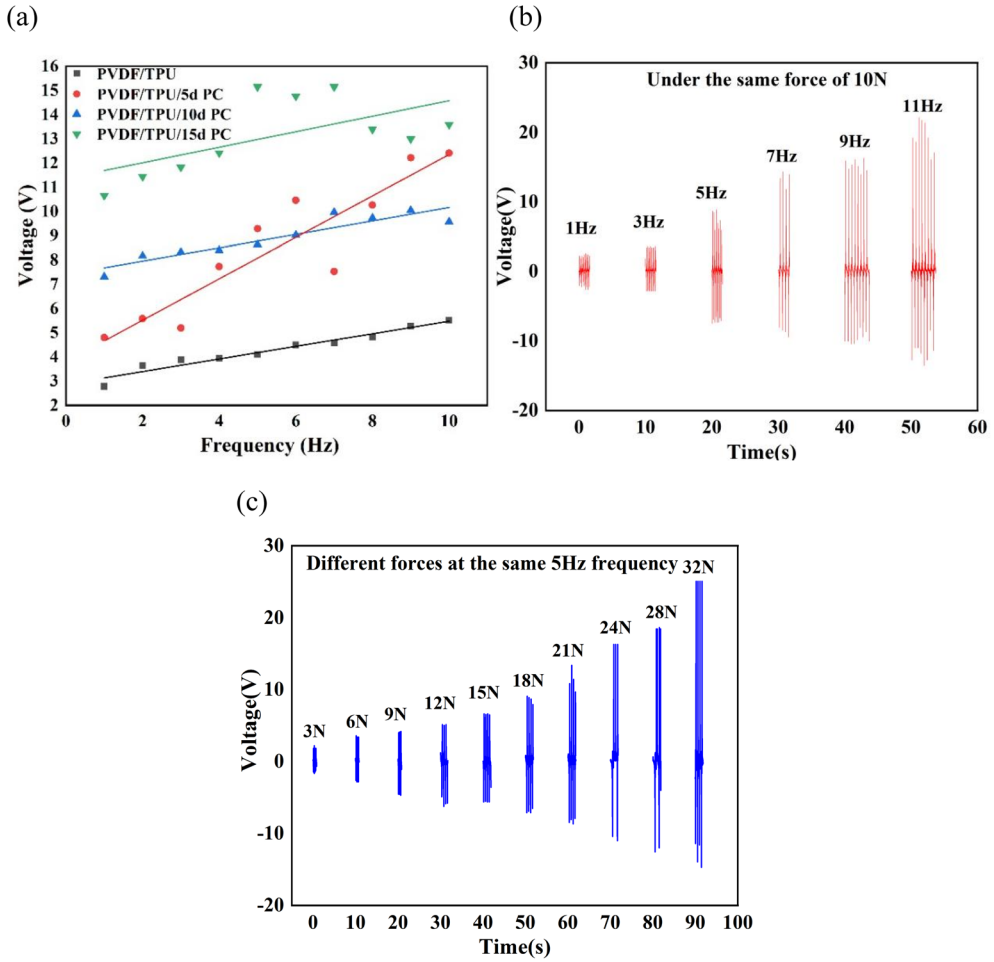

Fig. 9 Relation between peak-to-peak voltage and frequencies and different loads with the same frequency (a) peak voltage and frequencies and different loads (b) same load with different frequency (c) different loads with same frequency.

As shown in Fig. 10a, the relationship between force and output voltage can be observed. It can be concluded that as the force increases, the voltage generally shows an upward trend. When the addition amount of PCs is 15 drops, the output voltage increases more rapidly and the slope reaches the maximum. Specifically, when the amount of photonic crystals decreases to 5 drops, the voltage rises rapidly under a smaller force and the growth rate gradually slows down. When the addition amount is 15 drops and 10 drops, under a larger force, the voltage increases more quickly; significantly, when the force exceeds 25 N, the voltage rises. In the absence of photonic crystal addition, the growth is relatively gentle and the voltage value is generally lower. In summary, by adding photonic crystals, the output voltage is increased, demonstrating excellent piezoelectric performance, as shown in Fig. 9a.

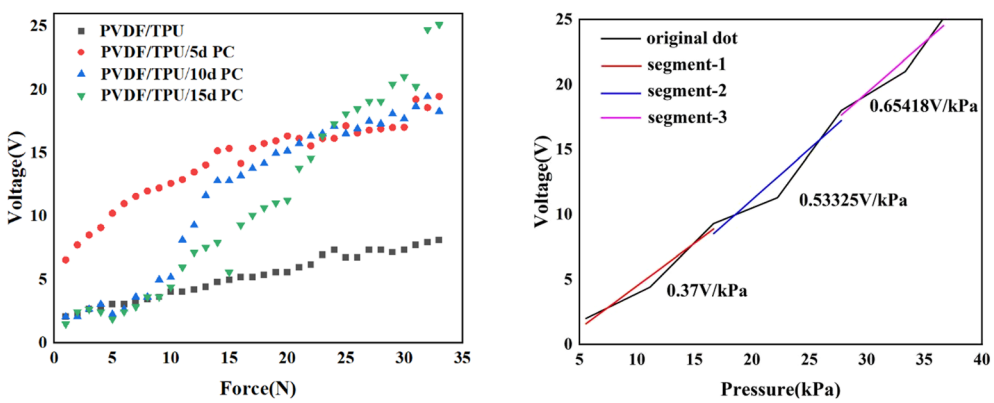

Fig. 10 Relation between peak-to-peak voltage and applied forces.

In Fig. 10b, the PENG's sensitivity to force is tested, and the output voltages at different pressures are presented. The PENG with PVDF/TPU/PC15d was selected for testing. The equidistant points in the detection range were selected for fitting, and the fitting equation and results are shown in Fig. 10b. The response voltage was well fitted within the range of 0–40 kPa, and the piecewise linear fitting had a good configuration. The pressure variation was relatively stable. Within the range of 0–40 kPa, the sensitivity reached 0.6845 V kPa^{-1}, and the sensitivity gradually increased with the increase of the applied pressure. The sensitivity curve can be divided into three stages: within the range of 0–11.11 kPa, it was 0.37 V kPa^{-1}; within the range of 11.11–22.22 kPa, it was 0.53325 V kPa^{-1}; and within the range of 22.22–36.67 kPa, it was 0.65418 V kPa^{-1}. As the applied pressure increased, the effective deformation became larger, and accordingly, the sensitivity improved.

Conclusion

In this work, we investigated the unique characteristics of piezoelectric elastic nanocomposite materials with three-dimensional photonic crystals. The synthesized nanofiber mats were composed of PVDF/TPU with PC. The piezoelectric performance is better with the nanocomposite attachment of PCs with TPU/PVDF, and the elasticity feature is related to the blended TPU. Our synthesized mats have been used to generate electric voltage under the effect of different mechanical excitations, such as mechanical stresses with both controlled forces and vibration frequencies, along with impulse loading *via* falling masses. The optimum piezoelectric response is found at a blending ratio of TPU between 5d and 15d of the PCs. And based on the output voltage and piezo-sensitivity. The performance of PVDF/TPU/PC15d is the best. For example, the sensitivity reaches 0.6845 V kPa^{-1}, the output voltage reaches 25 N, and its stability is also the best. Although the ratio of PVDF is reduced, the mechanical elasticity of blended TPU with photonic crystals causes an improvement in the piezoelectric response of the nanocomposite. This conclusion has been supported by different measurements of piezoelectric voltage at various amplitudes and frequencies of vibrational forces. This innovative elastic-piezo nanocomposite can be applied within energy harvesting membranes and wearable electronics.

Data availability

The data that support the findings of this study are available on request from the corresponding author.

Conflicts of interest

The authors have no conflict of interest.

Acknowledgements

This work was supported by National Key R&D Programme of China (2024YFB4600167) and National Natural Science Foundation of China (U24A20109).

References

1 J. Jurasz, F. Canales, A. Kies, M. Guezgouz and A. Beluco, A review on the complementarity of renewable energy sources: Concept, metrics, application and future research directions, *Sol. Energy*, 2020, **195**, 703–724.
2 S. D. Mahapatra, P. C. Mohapatra, A. I. Aria, *et al.*, Piezoelectric materials for energy harvesting and sensing applications: Roadmap for future innovative materials, *Adv. Sci.*, 2021, **8**, 2100864.
3 T. Vijayakanth, D. J. Liptrot, E. Gazit, *et al.*, Recent advances in organic and organic–inorganic hybrid materials for piezoelectric mechanical energy harvesting, *Adv. Funct. Mater.*, 2022, **32**, 2109492.
4 H. Zhou, *et al.*, Stretchable piezoelectric energy harvesters and self-powered sensors for wearable and implantable devices, *Biosens. Bioelectron.*, 2020, **168**, 112569.
5 Y. Liu, *et al.*, Piezoelectric energy harvesting for self-powered wearable upper limb applications, *Nano Sel.*, 2021, **2**, 1459–1479.
6 J. He, *et al.*, Wearable superhydrophobic PPy/MXene pressure sensor based on cotton fabric with superior sensitivity for human detection and information transmission, *Colloids Surf., A*, 2022, **642**, 128676.
7 F. Chen, *et al.*, High-sensitivity wearable multi-signal sensor based on self-powered MXene hydrogels, *Chem. Eng. J.*, 2024, **489**, 151221.
8 W. Yao, *et al.*, Mechanically durable superhydrophobic strain sensors with high biocompatibility and sensing performance for underwater motion monitoring, *ACS Appl. Mater. Interfaces*, 2024, **16**(5), 6548–6561.
9 N. Sezer and M. Koc, A comprehensive review on the state-of-the-art of piezoelectric energy harvesting, *Nano Energy*, 2020, **80**, 105567.
10 R. Atif, *et al.*, Solution blow spinning of polyvinylidene fluoride-based fibers for energy harvesting applications: A review, *Polymers*, 2020, **12**, 1304.
11 F. Wang, *et al.*, High-performance piezoelectric nanogenerator with silver nanowires embedded in polymer matrix for mechanical energy harvesting, *Ceram. Int.*, 2021, **47**, 35096–35104.
12 M. M. Rana, *et al.*, Porosity-modulated high-performance piezoelectric nanogenerator based on organic/inorganic nanomaterials for self-powered structural health monitoring, *ACS Appl. Mater. Interfaces*, 2020, **12**, 47503–47512.
13 T. Seesaard and C. Wongchoosuk, Flexible and stretchable pressure sensors: from basic principles to state-of-the-art applications, *Micromachines*, 2023, **14**(8), 1638.
14 A. Yadav, *et al.*, Fabrication of 3D polymeric photonic arrays and related applications, *Mater. Today Chem.*, 2020, **15**, 100208.
15 A. Yadav, *et al.*, Fabrication of self-assembled three-dimensional nano photonic crystals and potential applications, *Sci. Adv. Today*, 2017, **3**, 25275.

16 T. Dutta, *et al.*, Electronic properties of 2D materials and their junctions, *Nano Mater. Sci.*, 2024, **6**(1), 1–23.
17 X. Ding, *et al.*, Highly accurate wearable piezoresistive sensors without tension disturbance based on weaved conductive yarn, *ACS Appl. Mater. Interfaces*, 2020, **12**(31), 35638–35646.
18 W. Zhong, *et al.*, Ultra-sensitive piezo-resistive sensors constructed with reduced graphene oxide/polyolefin elastomer (RGO/POE) nanofiber aerogels, *Polymers*, 2019, **11**(11), 1883.
19 S. Sukumaran, S. Chatbouri, D. Rouxel, E. Tisserand, F. Thiebaud and T. B. Zineb, Recent advances in flexible PVDF-based/piezoelectric polymer devices for energy harvesting applications, *J. Intell. Mater. Syst. Struct.*, 2021, **32**, 746–780.
20 U. Jammalamadaka and K. Tappa, Recent Advances in Biomaterials for 3D Printing and Tissue Engineering, *J. Funct. Biomater.*, 2018, **9**, 22.
21 Z. U. Arif, M. Y. Khalid, R. Noroozi, A. Sadeghianmaryan, M. Jalalvand and M. Hossain, Recent advances in 3D-printed polylactide and polycaprolactone-based biomaterials for tissue engineering applications, *Int. J. Biol. Macromol.*, 2022, **218**, 930–968.
22 N. Sezer, Z. Evis and M. Koç, Additive manufacturing of biodegradable magnesium implants and scaffolds: Review of the recent advances and research trends, *J. Magnesium Alloys*, 2021, **9**, 392–415.
23 R. Lay, G. S. Deijs and J. Malmström, The intrinsic piezoelectric properties of materials: a review focusing on biological materials, *RSC Adv.*, 2021, **11**, 30657–30673.
24 A. Yadav, *et al.*, Wearable strain sensors: state-of-the-art and future applications, *Mater. Adv.*, 2023, **4**, 1444–1459.
25 W. Zhong, *et al.*, Breathable and large curved area perceptible flexible piezoresistive sensors fabricated with conductive nanofiber assemblies, *ACS Appl. Mater. Interfaces*, 2020, **12**(33), 37764–37773.
26 M. Salama, A. Hamed, S. Noman, G. Magdy, N. Shehata and I. Kandas, Boosting piezoelectric properties of PVDF nanofibers *via* embedded graphene oxide nanosheets, *Sci. Rep.*, 2024, **14**, 16484.
27 N. Shehata, R. Nair, R. Boualayan, I. Kandas, A. Masrani, E. Elnabawy, N. Omran, M. Gamal and A. H. Hassanin, Stretchable nanofibers of polyvinylidenefluoride (PVDF)/thermoplastic polyurethane (TPU) nanocomposite to support piezoelectric response *via* mechanical elasticity, *Sci. Rep.*, 2022, **12**, 8335.
28 Q. He, Y. Zeng, L. Jiang, G. Lu ZiyuWang, H. Kang, Li Pei, B. Bethers, S. Feng, L. Sun, P. Sun, G. Chen, J. Jin, R. J. YueHou, W. Xu, E. Olevsky and Y. Yang, Growing recyclable and healable piezoelectric composites in 3D printed bioinspired structure for protective wearable sensor, *Nat. Commun.*, 2023, **14**, 6477.
29 B. Kottathodi, I. Royaud, M. Ponçot, S. Thomas and D. Rouxel, A review on electrospun PVDF-based nanocomposites: Recent trends and developments in energy harvesting and sensing applications Sreelakshmi Moozhiyil Purushothaman, Maïté Fernandes Tronco, *Polymer*, 2023, **283**, 126179.
30 Md. Nahid Parvez Roni, *et al.*, Optimizing β-Phase Content in PVDF Membranes *via* Modification of Dope Solution with Citric Acid/Nano-TiO_2 Using Nonsolvent-Induced Phase Separation Method, *Polymers*, 2025, **17**(4), 481.
31 X.-W. Lin, P. Gajula, X.-shan Luo, M. Zhao, Xiao-bo Zhao and Ye Fan, Piezoelectric properties improvement in soft membrane with wet-spinning prepared barium titanate/polyvinylidenefluoride composites fiber, *Sci. Rep.*, 2025, **15**, 12887.
32 S. Ramakrishna, *An Introduction to Electrospinning and Nanofbers*, World Scientifc, 2005.
33 D. Zhang, h. Wu, C. R. Bowen and Y. Yang, Recent advances in pyroelectric materials and applications, *Small*, 2021, **17**, e2103960.
34 T.-W. Lu, L.-C. Wang, C.-H. Lai and Po-T. Lee, Strain shapes the light in a photonic crystal nanocavity, *Photonics Res.*, 2020, **8**(1), 24–31.
35 K. R. Sanjaya Dinuwan Gunawardhana, R. B. V. B. Simorangkir, G. B. McGuinness, M. Salauddin Rasel, L. A. Magre Colorado, S. S. Baberwal, T. E. Ward, B. O. Flynn and M. Shirley, CoyleThe Potential of Electrospinning to Enable the Realization of Energy-Autonomous 35. Wearable Sensing Systems, *ACS Nano*, 2024, **18**, 2649–2684.
36 K. K. Sappati, *et al.*, Piezoelectric polymer and paper substrates: a review, *Sensors*, 2018, **18**(11), 3605.